Eur. J. Mineral.
2011, **23**, 269–277
Published online February 2011

Afmite, $Al_3(OH)_4(H_2O)_3(PO_4)(PO_3OH)\cdot H_2O$, a new mineral from Fumade, Tarn, France: description and crystal structure

ANTHONY R. KAMPF[1,*], STUART J. MILLS[2], GEORGE R. ROSSMAN[3], IAN M. STEELE[4], JOSEPH J. PLUTH[4] and GEORGES FAVREAU[5]

[1] Mineral Sciences Department, Natural History Museum of Los Angeles County, 900 Exposition Blvd., Los Angeles, CA 90007, USA
*Corresponding author, e-mail: akampf@nhm.org
[2] Department of Earth and Ocean Sciences, University of British Columbia, Vancouver, BC, Canada V6T 1Z4
[3] Division of Geological and Planetary Sciences, California Institute of Technology, Pasadena, CA 91125, USA
[4] Department of the Geophysical Sciences, The University of Chicago, 5734 S. Ellis Ave., Chicago, IL 60637, USA
[5] 421 Avenue Jean Monnet, 13090 Aix-en-Provence, France

Abstract: The new mineral afmite, $Al_3(OH)_4(H_2O)_3(PO_4)(PO_3OH)\cdot H_2O$, is triclinic with space group $P\bar{1}$ and cell parameters $a = 7.386(3)$, $b = 7.716(3)$, $c = 11.345(4)$ Å, $\alpha = 99.773(5)$, $\beta = 91.141(6)$, $\gamma = 115.58(5)°$, $V = 571.6(3)$Å^3 and $Z = 2$. It occurs, sometimes in association with matulaite and variscite, in fractures and solution cavities in shale/siltstone at Fumade, Tarn, France. The formation is probably largely the result of remobilisation and crystallisation during low-temperature hydrothermal activity and/or weathering and ground water activity. Afmite forms in cockscomb aggregates of diamond-shaped tablets on {001}, ubiquitously contact-twinned on {001} and also commonly twinned by rotation on [010] with {010} and {1$\bar{1}$0} composition planes, forming star-like sixlings. The streak of the mineral is white, the luster is pearly, and the Mohs hardness is about 1½. The mineral is flexible, but not elastic, has an irregular fracture and three cleavage directions: {001} perfect, {010} and {1$\bar{1}$0} good. The measured density is 2.39(3) g/cm^3 and the calculated density is 2.391 g/cm^3 based upon the empirical formula. Optical properties (white light): biaxial (+), $\alpha = 1.554(1)$, $\beta = 1.558(1)$, $\gamma = 1.566(1)$, $2V_{meas.} = 70(5)°$ and $2V_{calc} = 71°$. Electron microprobe analyses provided Al_2O_3 40.20 and P_2O_5 38.84 wt% and CHN analyses provided H_2O 25.64 wt%, total 103.68 wt%. Normalized EMP analyses and water based on the structure yield Al_2O_3 36.41, P_2O_5 35.17 and H_2O 28.42, total 100.00 wt%. Infrared and Raman spectra were consistent with the PO_3OH, OH and H_2O as indicated by the crystal-structure determination. The strongest powder X-ray diffraction lines are [d_{obs}(Å),I_{obs},(*hkl*)]: 11.089,100,(001), 3.540,81,(0$\bar{1}$3,$\bar{1}\bar{1}$2), 5.484,79,(002,101), 2.918,60($\bar{1}$22), 3.089,33($\bar{1}$13,201), 4.022,30,(102,$\bar{1}$12), 6.826,23,(010). The crystal structure, solved from twinned data, ($R_1 = 10.4$ % for 1262 $F_o > 4\sigma F$ reflections) consists of chains of AlO_6 octahedra parallel to [110] in which edge-sharing octahedral dimers share corners with individual octahedra. Both PO_4 and PO_3OH tetrahedra link the chains into sheets parallel to {001} and the PO_4 tetrahedra further serve to link two sheets together into a thick slab in which tetrahedral (*T*) and octahedral (*O*) layers alternate, forming a *T-O-T-O-T* sandwich. The linkage between these sandwiches in the **c** direction is via hydrogen bonding with isolated H_2O groups in the interlayer region. Afmite is closely related structurally to the turquoise-group minerals and specifically to planerite. The recently described mineral kobokoboite probably has a closely related sheet structure.

Key-words: afmite, new mineral, crystal structure, acid phosphate, Al-phosphate, planerite, kobokoboite, Fumade, France.

1. Introduction

The new mineral described herein was discovered by one of the authors (GF) in the late 1990s in an unusual deposit at Fumade, France known for secondary phosphate phases (Gayraud, 2010; Lheur & Meisser, 2010). The name 'afmite' is for the Association Française de Microminéralogie (AFM). Founded in 1984 and with a current membership of over 430, AFM is one of the most active amateur associations in the domain of micro-minerals. Members of AFM have been responsible for the discovery of 21 new minerals: bariopharmacoalumite, bouazzerite, capgaronnite, deliensite, gatelite-(Ce), geminite, gilmarite, iltisite, jacquesdietrichite, lapeyreite, maghrebite, perroudite, pushcharovskite, rabejacite, radovanite, rouaite, theoparacelsite, tillmannsite, trimounsite-(Y), walkilldellite-(Fe) and yvonite. Members of AFM have actively collected the phosphate minerals of Fumade and are largely responsible for making the minerals of this locality known.

The mineral was originally submitted to the Commission on New Minerals and Mineral Names (CNMMN) [now reconstituted as the Commission on New Minerals, Nomenclature and

DOI: 10.1127/0935-1221/2011/0023-2093
0935-1221/11/0023-2093 $ 4.05

Classification (CNMNC)] of the International Mineralogical Association (IMA) in 2005 (IMA2005-025). Although the voting was predominantly positive, many delegates expressed concerns, causing the Chairman to suspend the voting. Among the concerns expressed were: (1) problems in rectifying the chemical analyses, density and unit cell leading to a proposed Z of 1.5; (2) lack of evidence for the presence of PO_3OH; and (3) the possibility that the mineral might actually be planerite (Foord & Taggart, 1998).

The current paper reports the results of a subsequent submission in 2010 (IMA2005-025a) in which all of these concerns were addressed and, most importantly, a crystal structure determination was reported, clearly defining the ideal formula of afmite, clarifying its relationship to planerite and shedding light on the likely relationship of kobokoboite (Mills *et al*., 2010) to both afmite and planerite. Based upon this second submission, the mineral and name have now been approved by the CNMNC. The holotype specimen has been deposited in the collections of the Natural History Museum of Los Angeles County, 900 Exposition Boulevard, Los Angeles, CA 90007, USA, catalogue number 55425.

2. Occurrence

Afmite is found at Fumade (hamlet), Castelnau-de-Brassac (village), Tarn, France (43°39′30″N, 2°29′58″E). Here, rocks containing the phosphate mineralisation are only exposed in ploughs in a farmer's field. The phosphates occur in fractures and solution cavities in shale/siltstone. Most of the specimens of afmite were collected from a few large blocks. Due to the brittle nature of the matrix, specimens rarely exceed 6 cm in length. Afmite coverage rarely exceeds one or two square centimetres.

Afmite is rarely associated with the Al-phosphates matulaite and variscite, but usually it is not directly associated with any other well-crystallised phosphate minerals. Afmite sometimes occurs on todorokite and other, poorly defined, manganese oxides. Other secondary phosphate species noted at the locality include wavellite, cacoxenite, beraunite and strengite.

The Cambrian age shale/siltstone was mildly metamorphosed during the Hercynian age intrusion of the Sidobre granite (Pierrot *et al*., 1976). Because of the limited exposures at the locality, it has not been possible to determine the source of the phosphate; however, it is presumed to have been present in the original sediments. While some recrystallisation of phosphates probably occurred during Hercynian metamorphism, the formation of afmite and the other secondary phosphate minerals is probably largely the result of remobilisation and crystallisation during more recent low-temperature hydrothermal activity and/or weathering and ground water activity.

We have also confirmed afmite to occur intergrown with kobokoboite at the Kobokobo pegmatite, Democratic Republic of Congo (Mills *et al*., 2010), and we have found afmite and/or kobokoboite to occur in association with matulaite, or misidentified as matulaite, on specimens from the Bachman mine, Hellertown, Pennsylvania, USA. Note that a manuscript reporting the crystal structure of matulaite based upon material from Fumade and Hellertown is in preparation. Based upon this study the ideal formula for matulaite is $(Fe^{3+},Al)Al_7(PO_4)_4(PO_3OH)_2(OH)_8(H_2O)_8\cdot 8H_2O$.

3. Crystal morphology

Crystals are thin diamond-shaped tablets on {001} with [010] elongation. Forms observed are {001}, {100}, {110} and {010}. Crystals exhibit ubiquitous contact twinning on {001}. Individual twinned tablets are up to 0.40 × 0.25 × 0.02 mm (Fig. 1 and 2). Tablets are also commonly twinned by rotation on [010] with {010} and $\{1\bar{1}0\}$ composition planes, forming star-like sixlings (Fig. 3), which are slightly concave/convex (dish-like). Tablets and sixlings commonly occur in cockscomb aggregates up to 1 mm across. The foregoing description of crystal morphology and twinning is based upon single-crystal X-ray diffraction (precession and diffractometer) and reflection-goniometer studies.

4. Physical and optical properties

Crystals typically exhibit a dull white to cream to yellowish surface, presumably from weathering. Freshly broken aggregates exhibit {001} faces that are colourless to white with a pearly lustre. The streak is white and the Mohs

Fig. 1. Cockscomb aggregates of diamond-shaped afmite tablets (FOV ~ 1 mm). Georges Favreau specimen.

Fig. 2. SEM image of afmite. Note diamond-shaped multiple crystal at lower left. Image by Bertrand Devouard, OPGC, Clermont-Ferrand, France.

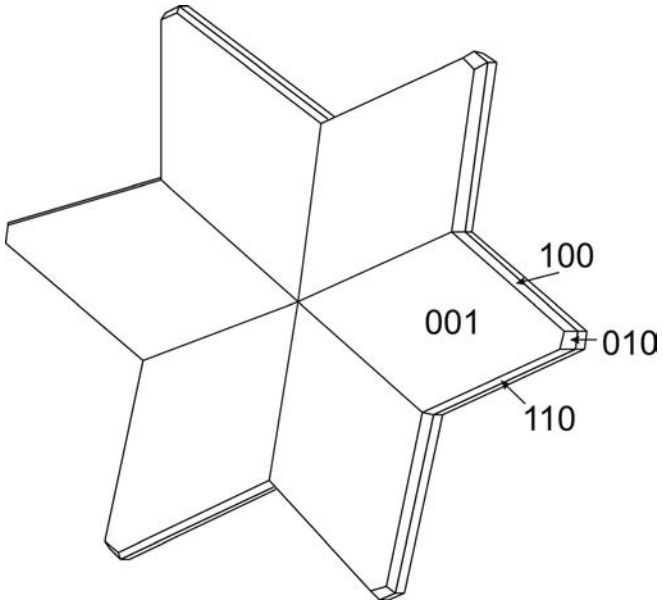

Fig. 3. Crystal drawing of afmite showing contact twinning on {001} and twinning by rotation on [010].

hardness is estimated to be about 1½. Thin crystal fragments are flexible, but not elastic. The fracture is irregular and there are three cleavage directions: {001} perfect, {010} and {1$\bar{1}$0} good. The mineral is non-fluorescent under all wavelengths of ultraviolet radiation. The density measured by sink-float in aqueous solution of sodium polytungstate is 2.39(3) g/cm^3. The calculated density, based on the empirical formula and single-crystal cell, is 2.391 g/cm^3 and that for the ideal formula is 2.394 g/cm^3.

The determination of the optical properties was complicated by the fact that contact twins on {001} could not be separated. A tablet exhibiting simple contact twinning was mounted on a Supper spindle stage on an Ortholux II polarising microscope. Extinction data were obtained for each individual of the contact twin, and analyses of these data using EXCALIBR (Gunter *et al*., 2004) for each of the twins yielded the orientations of the principal optic directions and the 2*V*. Afmite is biaxial (+) with indices of refraction, $\alpha = 1.554(1)$, $\beta = 1.558(1)$ and $\gamma = 1.566(1)$, measured in white light. The 2*V* obtained from the extinction data using EXCALIBR is 70(5)° and the 2*V* calculated from the indices of refraction is 71°. No pleochroism was observed. Because the unit cells of the respective twins could not be differentiated from the X-ray diffraction study, the optical orientation could not be completely determined. Plotting the unit-cell data for both cells along with the spindle-stage extinction curves on a Wulff net yielded the following relationships: $Y \approx \mathbf{a}$; **b** is at roughly equal angles (~55°) to *X* and *Z*. The Gladstone–Dale compatibility index $1 - (K_P/K_C)$ as defined by Mandarino (1981) provides a measure of the consistency among the average index of refraction, calculated density and chemical composition. For afmite, the compatibility index is 0.0121 (superior) based on the ideal formula and calculated density and 0.0103 (superior) based on the empirical formula and calculated density.

5. Infrared and Raman spectroscopy

The infrared spectra of afmite, kobokoboite and planerite were obtained with a Nicolet Magna860 FTIR and a SensIR DuraScope Attenuated Total Reflection (ATR) accessory and enough powdered mineral to cover a 1 mm diameter spot on the diamond ATR plate. One thousand scans at 4 cm^{-1} resolution were obtained for each mineral. The spectra are compared in Fig. 4. Planerite was chosen for its structural and chemical similarity with afmite. Kobokoboite was chosen because of its chemical similarity and the likelihood that it is structurally related to afmite and because it contains an acid phosphate group.

All three spectra are dominated by phosphate bending modes in the 550–600 cm^{-1} region and phosphate

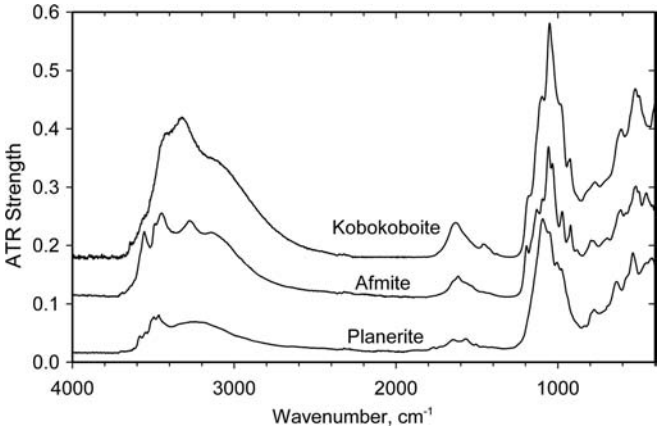

Fig. 4. Infrared ATR absorption spectrum of afmite compared with those of kobokoboite and planerite.

antisymmetric stretching modes in the 900–1200 cm^{-1} region. Also obvious are OH bands in the 3000–3600 cm^{-1} range and water bending modes around 1600 cm^{-1}. Considering the structural similarity of afmite and planerite (see crystal-structure discussion below), it is not surprising that their spectra are particularly similar.

The afmite spectrum has multiple bands in the OH region, both sharp and broad. The sharp bands more likely represent the OH groups associated with the aluminium, and the broad, underlying component comes from the molecular water. The successively higher contents of molecular water in planerite, afmite and kobokoboite are reflected in successively greater absorptions in the 3000–3600 and 1600 cm^{-1} ranges for each phase.

The PO_3OH groups commonly exhibit OH modes in the 2400–3300 cm^{-1} range, typically at lower energies than OH groups not associated with acid phosphates, due to stronger hydrogen bonding (Ross, 1974). The afmite and kobokoboite spectra exhibit significantly greater absorption in the 3000 cm^{-1} region, whereas the broad OH absorption is located at higher wave numbers in the planerite spectrum. Note that the extensive hydrogen bonding interaction with the water molecules makes it difficult to intuitively assign bands to particular OH groups.

The Raman spectrum of afmite was obtained with a Renishaw M1000 instrument with about 5 mW of 514 nm laser light on the sample with a 2 μm spot on the (001) face. Twenty scans with 30 s accumulations were averaged. The spectrum (Fig. 5) shows strong OH bands in the 3600–3000 cm^{-1} range from both water and OH groups, water bending near 1600 cm^{-1}, phosphate modes near 1000 cm^{-1}, and more complex modes at lower wave numbers. The multiplicity of bands in the phosphate region is consistent with the reduced symmetry of the PO_4 group from ideal tetrahedral geometry as indicated in Table 5.

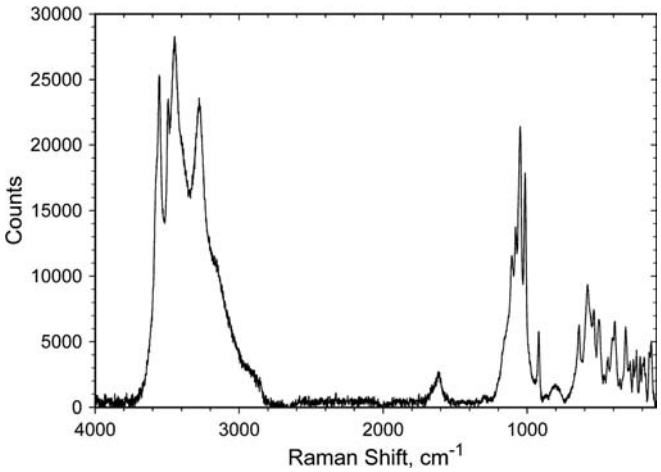

Fig. 5. Baseline corrected Raman spectrum of afmite.

6. Chemistry

Chemical analyses ($n = 4$) were carried out using a Cameca SX50 electron microprobe (WDS mode, 15 kV, 10 nA, and 10 μm beam diameter). Water determinations ($n = 2$) were carried out using a Carlo Erba element analyser. The water content from the CHN analysis is likely to be somewhat low because of minor amounts of manganese oxides, which could not be entirely removed from the crystals of afmite. The interlayer H_2O (see crystal structure section) is apparently very weakly held in afmite because the mineral is very prone to water loss during EMP analyses, which seems to occur simply from exposure to a vacuum. The water loss results in significantly high analytical amounts for Al and P. Using the H_2O content provided by the structural formula, we have normalised the EMP analyses for Al_2O_3 and P_2O_5 down ($\times 0.906$) to provide a 100 % total. The close match between the measured density and that calculated from the structural formula and also the superior Gladstone-Dale compatibility index based upon the structural formula supports this approach. The results are provided in Table 1.

7. X-ray crystallography and structure determination

Powder X-ray diffraction data were obtained on a Rigaku R-Axis Rapid II curved-imaging-plate microdiffractometer utilizing monochromatised Mo$K\alpha$ radiation. The powder data presented in Table 2 show good agreement with those calculated from the structure determination, although it should be noted that, due to the use of Mo$K\alpha$ radiation, numerous peaks predicted from the structure data (*e.g.*, 6.6086, 5.3502, 5.3228, 3.9468, 3.4811, 2.8809 and 2.8575) do not appear in the listing of the observed peaks because they are contained within the shoulders of adjacent larger peaks and cannot be discriminated as separate peaks. The close match between the observed and calculated powder data is more apparent when presented graphically, as shown in Fig. 6.

Ubiquitous fine-scale polysynthetic twinning and the general warping of crystals made the selection of a crystal fragment suitable for structure data collection very challenging. Data obtained on a small single-crystal fragment ($50 \times 40 \times 5$ μm) using synchrotron radiation were not of

Table 1. Analytical data for afmite.

Constituent	Wt%	Range	Std. dev.	Standard	Normalised Wt%
Al_2O_3	40.20	39.49–41.19	0.85	Anorthite	36.41
P_2O_5	38.84	37.58–39.87	0.94	$Ca_2P_2O_7$	35.17
H_2O	25.64[a]	25.09–26.19	0.78		28.42[b]
Total	103.68				100.00

[a]CHN analyses.
[b]Based on the structure.

Table 2. Observed and calculated X-ray powder-diffraction data for afmite.

I_{obs}	d_{obs}	d_{calc}	I_{calc}	*hkl*
100	11.089	11.0864	100	0 0 1
23	6.826	6.8063	30	0 1 0
		6.6086	10	1 0 0
20	6.431	6.3874	16	0 $\bar{1}$ 1
79	5.484	5.5432	36	0 0 2
		5.4307	52	1 0 1
		5.3502	9	0 1 1
		5.3228	14	$\bar{1}$ 1 1
8	4.365	4.3565	5	1 $\bar{1}$ 2
30	4.022	4.0426	7	1 0 2
		4.0147	20	$\bar{1}$ 1 2
		3.9468	10	$\bar{1}$ $\bar{1}$ 1
81	3.540	3.5539	16	0 $\bar{1}$ 3
		3.5241	47	$\bar{1}$ $\bar{1}$ 2
		3.4811	25	2 $\bar{1}$ 1
3	3.295	3.3043	9	2 0 0
7	3.201	3.1937	8	0 $\bar{2}$ 2
33	3.089	3.0852	12	$\bar{1}$ 1 3
		3.0792	32	2 0 1
8	2.992	2.9868	10	$\bar{2}$ 2 1
60	2.918	2.9165	40	$\bar{1}$ 2 2
		2.8809	11	1 $\bar{2}$ 3
		2.8575	13	2 $\bar{2}$ 2
12	2.558	2.5519	8	1 $\bar{3}$ 1
17	2.468	2.4650	11	1 0 4
4	2.364	2.3630	3	$\bar{1}$ 3 1
		2.3527	3	2 $\bar{3}$ 2
		2.3520	2	3 $\bar{2}$ 1
9	2.321	2.3153	7	$\bar{2}$ 2 3
12	2.280	2.2772	10	$\bar{2}$ $\bar{1}$ 3
		2.2755	4	1 $\bar{3}$ 3
7	2.216	2.2173	3	0 0 5
		2.2029	3	3 0 0
5	2.135	2.1310	6	$\bar{2}$ 3 2
6	2.079	2.0838	6	$\bar{1}$ 2 4
3	2.057	2.0604	4	1 $\bar{2}$ 5
		2.0528	3	1 $\bar{3}$ 4
16	1.982	1.9770	14	3 0 2
9	1.891	1.8866	10	$\bar{3}$ $\bar{1}$ 1
8	1.832	1.8301	6	$\bar{1}$ 0 6
18	1.771	1.7803	3	3 $\bar{4}$ 0
		1.7692	6	0 $\bar{3}$ 5
		1.7627	5	2 $\bar{3}$ 5
6	1.611	1.6107	5	4 $\bar{3}$ 3
9	1.545	1.5459	3	1 2 5
		1.5417	6	$\bar{2}$ 3 5
9	1.506	1.5050	4	3 $\bar{5}$ 1
18	1.493	1.4932	4	$\bar{2}$ $\bar{3}$ 4
		1.4898	2	$\bar{4}$ 0 4
		1.4894	3	3 $\bar{5}$ 0
18	1.456	1.4583	2	$\bar{2}$ 4 4
		1.4521	2	5 $\bar{2}$ 1
5	1.439	1.4382	5	0 $\bar{3}$ 7
10	1.310	1.3068	2	$\bar{2}$ $\bar{1}$ 8
		1.3066	1	$\bar{3}$ 2 7

Notes: I_{obs} and d_{obs} derived by profile fitting using JADE 9.1 software. I_{calc} and d_{calc} calculated from the crystal structure using Powder Cell (Kraus & Nolze, 1996). Only calculated reflections with intensities greater than 5 are included, unless they correspond to observed reflections. Unit-cell parameters refined from the powder data using JADE 9.1 with whole-pattern fitting are: $a = 7.373(11)$, $b = 7.699(11)$, $c = 11.334(12)$ Å, $\alpha = 99.80(3)$, $\beta = 91.20(3)$ and $\gamma = 115.61(5)°$.

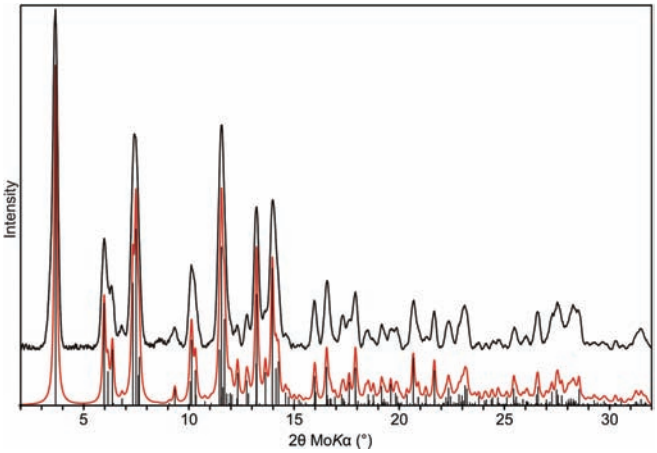

Fig. 6. Comparison of the observed powder X-ray diffraction pattern for afmite with that calculated from the structure. Individual calculated intensities are shown as vertical lines. The lower curve is simulated from the individual calculated intensities. The upper curve is the recorded pattern.

sufficient quality for structure determination. Data were subsequently collected on a larger crystal (100 × 80 × 10 μm), consisting of two individuals twinned by reflection on {001}, using the same Rigaku R-Axis Rapid II instrument noted above. The Rigaku CrystalClear software package, and specifically the TwinSolve program, was used for processing the structure data, including the application of an empirical absorption correction. A unit cell consistent with the synchrotron single-crystal cell was obtained. The structure was solved with SIR92 (Altomare *et al*., 1994) by direct methods using non-overlapping reflections. The SHELXL-97 software (Sheldrick, 2008) was used, with neutral atom scattering factors, for the refinement of the structure from the complete set of twinned data. The relatively high *R* factor, 10.4 %, is attributed to poor crystal quality and the imperfect nature of refinement using a twinned dataset. The data collection and structure refinement details are provided in Table 3, atomic coordinates and displacement parameters in Table 4, selected bond distances in Table 5 and bond valence summations in Table 6.

8. Discussion of the structure

The structure of afmite (Fig. 6) consists of chains of AlO_6 octahedra parallel to [110] in which edge-sharing octahedral dimers (Al1 Al2) share corners with individual octahedra (Al3). Both PO_4 (P2) and PO_3OH (P1) tetrahedra link the chains into sheets parallel to {001} (Fig. 7). The PO_4 tetrahedra further link two adjacent sheets together into a thick slab in which tetrahedral (*T*) and octahedral (*O*) layers alternate, forming a T–O–T–O–T sandwich (Fig. 8 and 9). The linkage between these sandwiches in the **c** direction is *via* hydrogen bonding with isolated H_2O groups in the interlayer region.

Table 3. Data collection and structure refinement details for afmite.

Diffractometer	Rigaku R-axis rapid II
X-ray radiation/power	Mo$K\alpha$ ($\lambda = 0.71075$ Å)/50 kV, 40 mA
Temperature	298(2) K
Ideal formula	$Al_3(OH)_4(H_2O)_3(PO_4)(PO_3OH)\cdot H_2O$
Space group	P-1
Unit-cell dimensions	$a = 7.386(3)$ Å
	$b = 7.716(3)$ Å
	$c = 11.345(4)$ Å
	$\alpha = 99.773(5)^\circ$
	$\beta = 91.141(6)^\circ$
	$\gamma = 115.58(5)^\circ$
Z	2
Volume	571.6(3) Å^3
Density (for formula above)	2.394 g/cm^3
Absorption coefficient	0.718 mm^{-1}
F(000)	420
Crystal size	100 × 80 × 10 μm
θ Range	1.84° to 20.04°
Index ranges	$0 \le h \le 7$, $-7 \le k \le 6$, $-10 \le l \le 10$
Reflections collected/ unique	1856/1856
Reflections with $F_o > 4\sigma F$	1262
Completeness to $\theta = 20.04^\circ$	96.7 %
Refinement method	Full-matrix least-squares on F^2
Parameters refined	193
GoF	1.108
Final R indices [$F_o > 4\sigma F$]	$R_1 = 0.1040$, w$R_2 = 0.2342$
R indices (all data)	$R_1 = 0.1468$, w$R_2 = 0.2554$
Extinction coefficient	0.032(10)
Largest diff. peak/hole	+0.656/–0.644 e/A^3

Notes: $R_{int} = \sum|F_o^2 - F_o^2(\text{mean})|/\sum[F_o^2]$. GoF = $S = \{\sum[w(F_o^2 - F_c^2)^2]/(n-p)\}^{1/2}$. $R_1 = \sum||F_o| - |F_c||/\sum|F_o|$. $wR_2 = \{\sum[w(F_o^2 - F_c^2)^2]/\sum[w(F_o^2)^2]\}^{1/2}$. $w = 1/[\sigma^2(F_o^2) + (aP)^2 + bP]$ where a is 0.1073, b is 7.2091 and P is $[2F_c^2 + \text{Max}(F_o^2, 0)]/3$.

Afmite is closely related structurally to the turquoise group minerals and specifically to planerite, which evidently possesses the turquoise structure (Kolitsch & Giester, 2000) with vacancies at the Cu sites (Fig. 9). The planerite structure has the same octahedral chains, linked in the same way by phosphate tetrahedra into sheets. The structures differ in that the sheets in planerite are linked into a framework via octahedral-tetrahedral corners. Interestingly, the linkage between the sheets in planerite is *via* the same tetrahedral corner that is the OH of the PO_3OH tetrahedron of afmite.

Foord & Taggart (1998) provide the ideal formula for planerite as $Al_6(PO_4)_2(PO_3OH)_2(OH)_8\cdot 4H_2O$ and note that the acid phosphate group is necessary to balance the net negative charge resulting from the vacancy in the Cu site of the turquoise structure. However, because all phosphate O atoms in the turquoise structure type are also bonded to Al^{3+}, bond valence considerations suggest that no specific phosphate O atoms in planerite are OH. Also, in relation to the IR spectra as noted above, absorption in the 2400–3300 cm^{-1} range that is typical of OH modes associated with PO_3OH groups is much less prominent in the spectrum of planerite than in the spectra of both afmite and kobokoboite. Although it is possible that one or more phosphate O atoms have some OH character, we suggest that it is more likely that the non-phosphate OH sites have some H_2O character and that, therefore, it is better to give the ideal formula for planerite as $\square Al_3(OH)_3(H_2O)_2(PO_4)_2$. It must be acknowledged, however, that without the determination of the crystal structure of planerite, the evidence supporting either formula is inconclusive.

Afmite, planerite and kobokoboite have the same Al:P ratio (3:2) and share similar a and b cell lengths and the angle γ between them (Table 7): 7.4–7.5, 7.7–7.8 Å and

Table 4. Atomic coordinates and displacement parameters for afmite.

	x	y	z	U_{eq}	U_{11}	U_{23}	U_{33}	U_{23}	U_{13}	U_{12}
Al1	0.1864(8)	0.8305(6)	0.7126(5)	0.026(2)	0.031(4)	0.008(3)	0.035(4)	0.011(3)	0.004(3)	0.004(3)
Al2	0.2134(7)	0.4544(7)	0.6879(5)	0.024(2)	0.019(3)	0.031(3)	0.022(3)	0.007(3)	0.001(2)	0.011(3)
Al3	0.3042(7)	0.8575(7)	0.2972(5)	0.018(1)	0.012(3)	0.017(3)	0.022(3)	0.005(2)	0.004(2)	0.003(2)
P1	0.3282(6)	0.1414(6)	0.5440(4)	0.018(1)	0.017(3)	0.014(3)	0.022(3)	0.001(2)	0.001(2)	0.007(2)
P2	0.0633(7)	0.1507(7)	0.8565(4)	0.027(2)	0.022(3)	0.027(3)	0.029(3)	0.005(2)	0.006(2)	0.008(2)
O1	0.1858(16)	0.9718(16)	0.5971(10)	0.024(3)	0.014(6)	0.051(8)	0.018(7)	0.021(6)	0.010(5)	0.020(6)
O2	0.3240(16)	0.0802(16)	0.4091(11)	0.030(3)	0.010(7)	0.040(7)	0.031(8)	0.009(6)	0.011(6)	0.002(6)
O3	0.5444(18)	0.2156(14)	0.6007(10)	0.031(3)	0.048(9)	0.017(6)	0.034(8)	0.003(6)	−0.002(7)	0.019(7)
O4	0.2677(15)	0.3112(15)	0.5576(10)	0.022(3)	0.022(7)	0.032(7)	0.021(7)	0.013(5)	−0.011(5)	0.019(6)
O5	0.2163(16)	0.3095(13)	0.8013(10)	0.020(3)	0.029(7)	0.000(5)	0.031(7)	0.004(5)	0.005(6)	0.005(5)
O6	0.1041(16)	0.9730(15)	0.8389(10)	0.024(3)	0.030(7)	0.026(6)	0.032(8)	0.015(6)	0.011(6)	0.024(6)
O7	0.8437(14)	0.0943(14)	0.8169(10)	0.016(3)	0.010(7)	0.017(6)	0.032(7)	0.020(5)	0.016(5)	0.009(5)
OH8	0.1061(15)	0.2342(14)	0.9962(10)	0.021(3)	0.020(7)	0.015(6)	0.026(7)	0.005(5)	−0.001(5)	0.005(5)
OH9	0.2352(17)	0.6431(15)	0.6019(10)	0.027(3)	0.038(8)	0.032(7)	0.031(8)	0.006(6)	0.014(6)	0.032(6)
OH10	0.9288(16)	0.3042(15)	0.6407(10)	0.027(3)	0.021(7)	0.025(6)	0.027(8)	0.008(6)	0.010(6)	0.002(6)
OH11	0.1502(15)	0.6327(14)	0.8078(10)	0.022(3)	0.015(6)	0.013(6)	0.035(8)	0.015(5)	0.002(6)	−0.001(5)
OH12	0.4622(16)	0.9848(16)	0.7763(11)	0.034(3)	0.013(7)	0.030(7)	0.037(8)	−0.003(6)	0.014(6)	−0.006(6)
OW13	0.5098(16)	0.6040(16)	0.7443(10)	0.027(3)	0.022(7)	0.035(7)	0.020(7)	0.001(6)	−0.003(6)	0.012(6)
OW14	0.8918(16)	0.6597(13)	0.6523(10)	0.026(3)	0.018(7)	0.005(6)	0.038(8)	0.004(5)	0.008(6)	−0.011(5)
OW15	0.2589(16)	0.6128(15)	0.1767(11)	0.029(3)	0.031(7)	0.026(7)	0.050(9)	0.022(6)	0.018(6)	0.027(6)
OW16	0.4778(19)	0.7673(18)	0.9921(12)	0.052(4)	0.043(9)	0.048(9)	0.043(9)	0.005(7)	0.005(7)	0.001(7)

Table 5. Selected bond lengths (Å) in afmite.

Al1–O1	1.835(11)	P1–O5	1.501(12)	Hydrogen bonding	
Al1–OH12	1.904(13)	P1–O6	1.506(10)	D–A	
Al1–OH9	1.907(11)	P1–O7	1.518(11)	OH8–O6	2.72(1)
Al1–O6	1.922(11)	P1–OH8	1.572(12)	OH9–O3	2.92(1)
Al1–OH11	1.940(10)	<P1–O>	1.524	OH10–O1	2.98(1)
Al1–OW14	2.019(12)			OH11–OW16	2.85(2)
<Al1–O>	1.921	P2–O1	1.508(12)	OH12–OW16	2.87(2)
		P2–O2	1.515(13)	OW13–O2	3.06(2)
Al2–OH9	1.834(11)	P2–O3	1.524(13)	OW13′–OH12	3.06(2)
Al2–O5	1.841(11)	P2–O4	1.539(10)	OW14–O4	2.71(1)
Al2–O4	1.845(12)	<P2–O>	1.522	OW14′–OH10	2.85(1)
Al2–OH10	1.916(12)			OW15–OH11	2.81(2)
Al2–OH11	1.974(11)			OW15′–OH8	3.00(1)
Al2–OW13	2.006(12)			OW16–OH11	2.85(2)
<Al2–O>	1.903			OW16′–OH12	2.87(2)
Al3–O7	1.855(11)				
Al3–OH10	1.868(12)				
Al3–O3	1.898(12)				
Al3–O2	1.900(12)				
Al3–OH12	1.929(12)				
Al3–OW15	2.022(12)				
<Al3–O>	1.912				

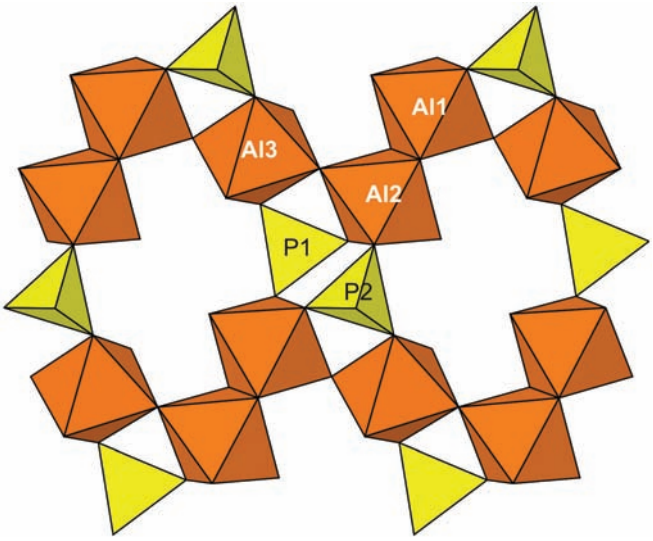

Fig. 7. Single sheet in afmite viewed parallel to {001} with the octahedral chain direction, [110], horizontal.

Table 6. Bond-valence summations for afmite.

	Al1	Al2	Al3	P1	P2	H-bonds	Σ
O1			0.51		1.24	+0.11	1.86
O2	0.61				1.30	+0.07	1.98
O3			0.51		1.27	+0.13	1.91
O4		0.59			1.19	+0.20	1.98
O5		0.60		1.32			1.92
O6	0.48			1.30		+0.20	1.98
O7			0.58	1.26			1.84
OH8				1.09		−0.20	0.99
						+0.10	
OH9	0.50	0.61				−0.13	0.98
OH10		0.49	0.56			−0.11	1.10
						+0.16	
OH11	0.46	0.42				−0.16	1.05
						+0.17	
						+0.16	
OH12	0.51		0.47			−0.15	1.05
						+0.07	
						+0.15	
OW13		0.38				−0.07	0.24
						−0.07	
OW14	0.37					−0.20	0.01
						−0.16	
OW15			0.37			−0.17	0.10
						−0.10	
OW16						−0.16	0.00
						−0.15	
						+0.16	
						+0.15	
Σ	2.93	3.09	3.00	4.97	5.00		

Notes: Non-hydrogen bond strengths from Brese & O'Keeffe (1991); hydrogen bond strengths from Ferraris & Ivaldi (1988), based on O–O distances; valence summations are expressed in valence units.

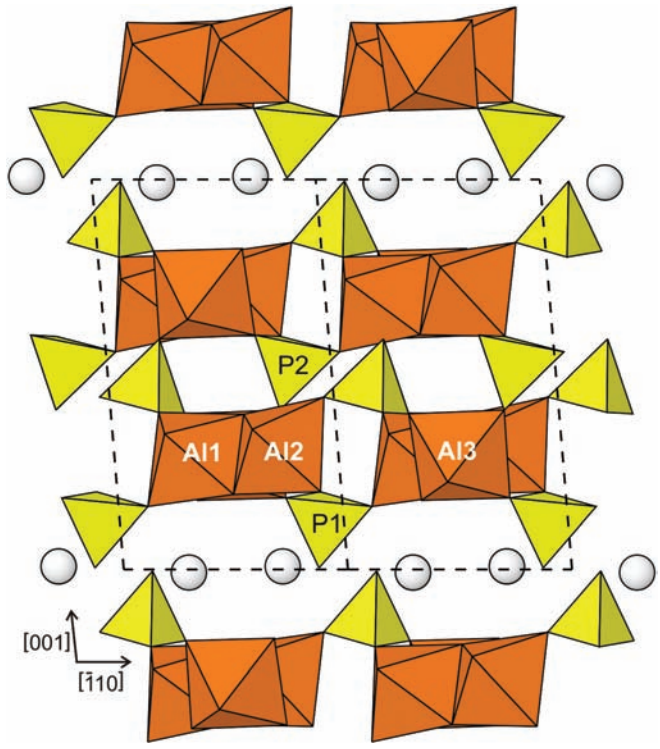

Fig. 8. Crystal structure of afmite viewed along the [110] octahedral chain direction. The O atoms of the interlayer H_2O groups are shown as spheres.

115–116°. These parameters in afmite and planerite are determined by the linkages of octahedra and tetrahedra forming their sheets parallel to {001}. Therefore, it is very likely that the structure of kobokoboite is based upon the same type of sheet of octahedra and tetrahedra

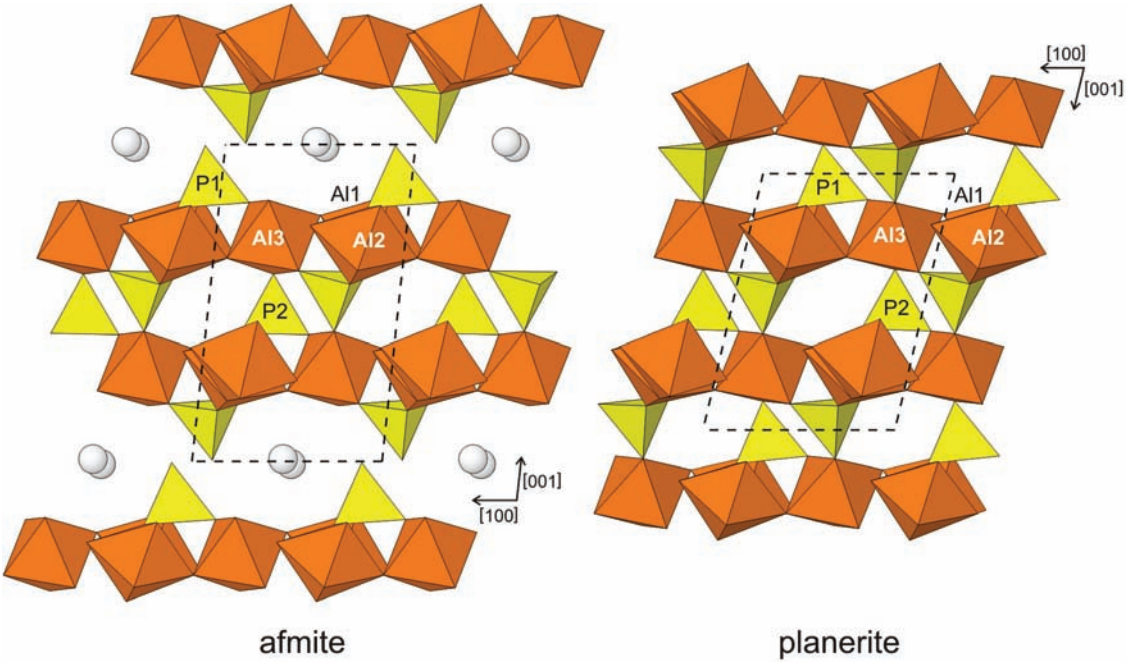

Fig. 9. Crystal structures of afmite and planerite viewed along [010]. The O atoms of the interlayer H_2O groups are shown as spheres.

Table 7. Comparison of selected data for planerite, afmite, and kobokoboite.

	Planerite[a]	Afmite	Kobokoboite[b]
Formula	$\square Al_3(OH)_3(H_2O)_2(PO_4)_2$	$Al_3(OH)_4(H_2O)_3(PO_4)(PO_3OH)\cdot H_2O$	$Al_6(PO_4)_4(OH)_6 11H_2O$
Crystallography			
Space group	*P*-1	*P*-1	*P*1 or *P*-1
a (Å)	7.505(2)	7.386(3)	7.460(1)
b (Å)	7.814(2)	7.716(3)	7.737(1)
c (Å)	9.723(3)	11.345(4)	12.385(5)
α (°)	111.43	99.773(5)	102.79(2)
β (°)	68.69	91.141(6)	90.20(3)
γ (°)	115.56	115.58(5)	116.33(2)
V (Å^3)	464.2(1)	571.6(3)	620.6(3)
Z	2	2	1
Chemistry (ideal)			
Al_2O_3 (wt%)	40.68	37.12	36.33
P_2O_5 (wt%)	37.76	34.45	33.71
H_2O (wt%)	21.56	28.42	29.96
Optics			
Optical class	Biaxial (+)	Biaxial (+)	Biaxial (–)
α	*n* ~1.60	1.554(1)	~1.550
β		1.558(1)	1.558(2)
γ		1.566(1)	1.562(2)
$2V_{meas}$ (°)	nd	70(5)	large, 60–80
Other properties			
D_{meas}, D_{calc} (g/cm^3)	2.68(5), 2.71(5)	2.39(3), 2.394	2.21(3), 2.287
Colour	White, pale blue or pale green	Colourless	Colourless to white

[a]Foord & Taggert (1998). The cell has been transposed to correspond to the cells of turquoise, afmite and kobokoboite.
[b]Mills *et al*. (2010). The ideal formula provided is based upon the hypothetical structure.

parallel to {001} and that it differs from afmite and planerite in the linkage of sheets in the **c** direction.

Acknowledgements: Chief Editor Roland Oberhänsli and reviewers Peter Elliot and especially Andrew M. McDonald are thanked for helpful comments that significantly improved the paper. Jochen Schlueter is acknowledged for his assistance in arranging the CHN analysis at the University of Hamburg. This study was funded, in part, by the John Jago Trelawney Endowment to the Mineral Sciences Department of the Natural History Museum of Los Angeles County and the White Rose Foundation at Caltech. The first set of structure data was collected at ChemMatCARS, Sector 15, Advanced Photon Source at Argonne National Laboratory. ChemMatCARS Sector 15 is principally supported by the National Science Foundation/Department of Energy under grant number CHE-0535644. Use of the Advanced Photon Source was supported by the U.S. Department of Energy, Office of Science, Office of Basic Energy Sciences, under contract no. DE-AC02-06CH11357.

References

Altomare, A., Cascarano, G., Giacovazzo, C., Guagliardi, A., Burla, M.C., Polidori, G., Camalli, M. (1994): SIR92 – a program for automatic solution of crystal structures by direct methods. *J. Appl. Crystallogr.*, **27**, 435.

Brese, N.E. & O'Keeffe, M. (1991): Bond-valence parameters for solids. *Acta Crystallogr.*, **B47**, 192–197.

Ferraris, G. & Ivaldi, G. (1988): Bond valence vs. bond length in O. . .O hydrogen bonds. *Acta Crystallogr.*, **B44**, 341–344.

Foord, E.E. & Taggart, J.E., Jr. (1998): A re-examination of the turquoise group: the mineral aheylite, planerite (redefined), turquoise and coeruleolactite. *Mineral. Mag.*, **62**, 93–111.

Gayraud, L. (2010): Gisement de phosphates de Castelnau-de-Brassac aux environs de Fumade (Tarn). *Cah. Micromonteurs*, **107**, 12–17.

Gunter, M.E., Bandli, B.R., Bloss, F.D., Evans, S.H., Su, S.-C., Weaver, R.. (2004): Results from a McCrone spindle stage short course, a new version of EXCALIBR, and how to build a spindle stage. *Microscope*, **52**, 23–39.

Kolitsch, U. & Giester, G. (2000): The crystal structure of faustite and its copper analogue turquoise. *Mineral. Mag*., **64**, 905–913.

Kraus, W. & Nolze, G. (1996): POWDER CELL – a program for the representation and manipulation of crystal structures and calculation of the resulting X-ray powder patterns. *J. Appl. Crystallogr*., **29**, 301–303.

Lheur, C. & Meisser, N. (2010): Découverte de minéraux rares à Castelnau-de-Brassac (Tarn). *Le Règne minéral*, **91**, 46.

Mandarino, J.A. (1981): The Gladstone-Dale relationship: Part IV. The compatibility concept and its application. *Can. Mineral*., **19**, 441–450.

Mills, S.J., Birch, W.D., Kampf, A.R., van Wambeke, L. (2010): Kobokoboite, $Al_6(PO_4)_4(OH)_6\cdot 11H_2O$, a new mineral from the Kobokobo pegmatite, Democratic Republic of Congo. *Eur. J. Mineral*., **22**, 305–308.

Pierrot, R., Picot, P., Fortuné, J.-P., Tollon, F. (1976): Inventaire Minéralogique de la France N° 6: Tarn, BRGM ed., 27 (in French).

Ross, S.D. (1974): Phosphates and other oxy-anions of Group V. *in* ''The Infrared Spectra of Minerals'', V.C. Farmer, ed., **4**, *Mineral. Soc. Monograph*, chapter 17.

Sheldrick, G.M. (2008): A short history of *SHELX*. *Acta Crystallogr*, **A64**, 112–122.

Received 13 October 2010
Modified version received 11 January 2011
Accepted 13 January 2011